

Strongly Correlated Quantum Gas Prepared by Direct Laser Cooling

Pablo Solano,¹ Yiheng Duan,¹ Yu-Ting Chen,^{1,2}
Alyssa Rudelis,¹ Cheng Chin,³ and Vladan Vuletić^{1,*}

¹*Department of Physics, MIT-Harvard Center for Ultracold Atoms,
and Research Laboratory of Electronics,
Massachusetts Institute of Technology,
Cambridge, Massachusetts 02139, USA*

²*Department of Physics, Harvard University,
Cambridge, Massachusetts, 02138, USA*

³*James Franck Institute, Enrico Fermi Institute, Department of Physics,
University of Chicago, Chicago, Illinois 60637, USA*

(Dated: October 1, 2019)

* Corresponding author email: vuletic@mit.edu

I. SUPPLEMENTARY MATERIAL: FAST PREPARATION OF A SUPER-TONK GAS BY LASER COOLING

A. Experimental Details

^{133}Cs atoms are loaded from a magneto-optical trap (MOT) into a standing-wave trap operated at wavelength $\lambda = 1064$ nm with waist $w_x = 17$ μm and 100 mW of power (x -trap). The lattice is created by a vertically polarized beam and its retroreflection with the polarization rotated by about 83° , set to obtain trapping frequencies of $\omega_x = 2\pi \times 50$ kHz along the lattice and $\omega_{\perp x} = 2\pi \times 1.5$ kHz transverse to the beam propagation, with a calculated trap depth of $U_x/h = 2.2$ MHz. After loading into the trap and polarization gradient cooling to a temperature of $T=6$ μK , the phase space density (PSD, defined below) is $\text{PSD} \simeq 4 \times 10^{-3}$ [1], and the peak density is $n_0 \simeq 2 \times 10^{13} \text{cm}^{-3}$. We then perform degenerate Raman sideband cooling (dRSC) of the 2D gas by applying a magnetic field of about 150 mG to match the energy of the $|\nu; 6S_{1/2}, F = 3, m_F = 3\rangle$ and $|\nu - 1; 6S_{1/2}, 3, 2\rangle$ states, where ν represents the vibrational level of an atom in the direction of tight confinement. In this configuration the trapping light drives the $|\nu; 6S_{1/2}, F = 3, m_F = 3\rangle \rightarrow |\nu - 1; 6S_{1/2}, F = 3, m_F = 2\rangle$ Raman transition, with calculated Rabi frequency of $2\pi \times 2$ kHz. Unlike previous realizations of laser cooling to quantum degeneracy in ^{87}Rb [2, 3], we use light resonant with the $|6S_{1/2}, F=3\rangle \rightarrow |6P_{3/2}, F'=2\rangle$ transition to optically pump the atoms from the $|3, 2\rangle$ state back to $|3, 3\rangle$ using spontaneous Raman scattering, removing entropy from the system (see Fig. 1b of the main text for the atomic level structure). The pump light, with an intensity of 6 $\mu\text{W}/\text{cm}^2$, is mostly σ^+ polarized with a small component of π -light, to empty all magnetic sublevels other than the lowest-energy state $|3, 3\rangle$. At the end of this first cooling stage after 100 ms, the trap contains $N = 4000$ atoms with a peak occupancy of $N \simeq 90$ atoms per lattice site at a temperature of $T=2.5$ μK . At this point we have reached $\text{PSD} \sim 0.1$, and if we continue the cooling in this geometry, we observe that the PSD decreases due to the strong light-induced atom loss.

To prepare the atoms in a quasi-1D trapping geometry we proceed as follows: we adiabatically turn on a second lattice trap (y -trap) transverse to the first one with $w_y = 6.5$ μm waist and detuned from the x -trap by 160 MHz. This configuration creates a two dimensional array of elongated cigar-shaped traps along the z direction (see Fig. 1 of the main

text). This second lattice is created by a vertically polarized beam and its retroreflection with polarization rotated by 70° . We use 5.5 mW of power to achieve trapping frequencies of $\omega_y = 2\pi \times 50$ kHz along the lattice and $\omega_{\perp y} = 2\pi \times 2.5$ kHz transverse to it, with a calculated trap depth of $U_y/h = 0.47$ MHz.

Before the y -trap turns on, the cold atoms in the x -trap are distributed at the bottom of the potential with a root-mean-square radius of $1.3 \mu\text{m}$ in the y -direction, so that most of the atoms are loaded into 3 lattice sites along the y -trap (see Fig. 1a of the main text for reference to the coordinate system and Fig. 1c for the trap geometry). Immediately after switching on the y -trap, we adiabatically turn off the x -trap while increasing the power of the y -trap, allowing us to further compress the atoms in the x -direction, and to remove the atoms that are not confined to the overlap region of the two traps. The y -trap power is then increased by a factor of ten, producing a transverse frequency of $\omega_{\perp yc} = 2\pi \times 8$ kHz. At this point the temperature of the atoms has risen to about $20 \mu\text{K}$, leading to a root-mean-square cloud size of $0.7 \mu\text{m}$ along x . After 10 ms of thermalization the x -trap is adiabatically turned on. Finally, the y -trap power is adiabatically ramped back down to its previous value (Fig. 1c of the main text). The entire process of compressing the atoms along both lattices takes 40 ms, without significant reduction of the PSD. At the end of this stage we have about 1000 atoms at $5 \mu\text{K}$ distributed in a 2D array with rms size $\sim 1.3 \times 2.5$ lattice sites in the x and y directions, respectively, obtaining a peak occupation of $N \simeq 50$ atoms per cigar-shaped trap.

The final cooling stage follows the same dRSC scheme as the pre-cooling stage, but now in two dimensions (x and y). The trapping frequencies are $\omega_{x,y} = 2\pi \times 50$ kHz in the transverse directions and $\omega_z = \sqrt{\omega_{\perp x}^2 + \omega_{\perp y}^2} = 2\pi \times 2.9$ kHz along the weakly confined vertical direction. After 200 ms of cooling, we reach a kinetic energy of the free expansion that corresponds to the ground-state kinetic energy of the tightly confined direction, i.e. we cool to the 2D ground state in the xy -plane. During cooling, atoms are lost at a moderate rate due to light-assisted inelastic collisions; once the atoms are cooled to the 2D ground state, the loss rate substantially reduces, presumably due to the lower cooling and associated optical pumping rates.

The loss during the cooling is due to two-body collisions, with more loss occurring in the traps in the central region containing initially more atoms. We simulate the atom number distribution in each trap at fixed total loss for the ensemble during the final cooling

Trap wavelength	1064 nm
x -beam power	100 mW
y -beam power	5.5 mW
x -beam waist	17 μm
y -beam waist	6.5 μm
$\omega_{x,y}$	$2\pi \times 50$ kHz
ω_z	$2\pi \times 2.9$ kHz
Trap depth U	$\hbar \times 2.7$ MHz
Magnetic field B	0.15 G

TABLE I. Experimental parameters.

($N_{\text{initial}} = 1000$ atoms and $N_{\text{final}} = 300$ atoms), and find that this leads to a rather flat distribution in atom number, with most traps containing $N_1 = 6$ atoms.

B. Atom Number Distribution

During the last stage of cooling the atoms are lost mainly due to light-induced collisions, which for a given laser intensity and detuning depend on the probability of finding two atoms near each other while one of the atoms is not in the dark state $|F = 3, m = 3\rangle$. We can model light-induced losses as a two-body process, where the reduction of the number of atoms is given by the solution of the differential equation $\dot{N} = -\alpha N^2$, namely

$$N(t) = \frac{N_0}{\alpha N_0 t + 1}. \quad (1)$$

Here N_0 is the initial number of atoms and α is light-assisted two-body loss rate. We model the density profile of the atoms remaining in the trap by starting with a Gaussian distribution and letting it evolve following Eq. (1). Fig. 1 shows the evolution during cooling of $N_{\text{initial}} = 1000$ atoms in a Gaussian distribution with a width given by the geometric average of the rms size of the sample after compression in the x and y direction ($\sqrt{0.7\mu\text{m} \times 1.3\mu\text{m}}$), which corresponds to 1.8 lattice sites. By the time the atoms are cooled down to the transverse ground state there are about $N_{\text{final}} = 300$ atoms. In this case we predict an almost flat density distribution of about 50 tubes in two dimensions with 6 atoms per tube. The atoms contained in tubes outside the flat distribution make up about 20% of the signal.

Moreover, due to the low atom number they are expected to contribute very little to the two- and three-body correlation signals.

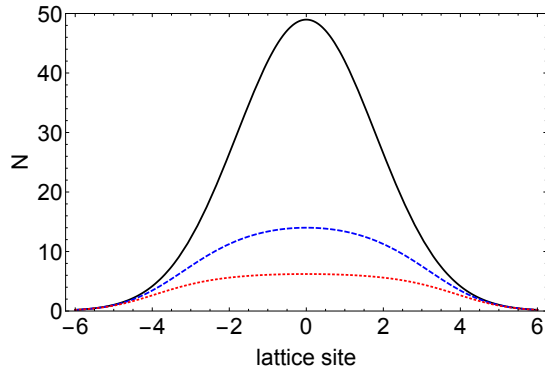


FIG. 1. Atom number distribution per lattice site at different cooling times. After loading into the 2D array of traps, the ensemble contains a 1000 atoms in a Gaussian distribution of the atom number per lattice site (solid black). As the atom number in each trap is reduced by two-body loss to a distribution with 500 atoms (dashed blue) and 300 atoms (dotted red), the nonlinearity of the loss leads to a flat distribution of atom numbers.

C. Magnetic Field Dependence

We apply a magnetic field rotated from the y axis by a small angle α . To optimize the optical pumping into the $|6S_{1/2}, F = 3, m_F = 3\rangle$ state, we scan the angle α by minimizing the atom loss at large optical pumping power. For the thusly obtained angle $\alpha \approx 10^\circ$, Fig. 2 shows the performance of dRSC versus magnetic field. We observe that the minimum temperature is reached near $B = 150$ mG, consistent with a Zeeman frequency splitting that equals the trapping frequency $\omega_{x,y}$ in the directions of tight confinement.

D. Calculation of Phase Space Density

The (classical) phase space density is defined as the probability for a single atom to populate the three-dimensional quantum ground state of the system, multiplied by the number of atoms per trap N_1 ,

$$\text{PSD} = N_1 P_0 = N_1 p_{0,x} p_{0,y} p_{0,z}, \quad (2)$$

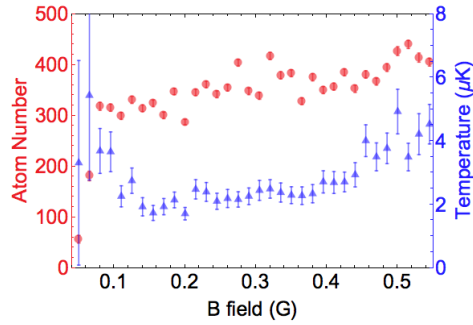


FIG. 2. Number of atoms (red circles) and temperature (blue triangles) as a function of magnetic field after 100 ms of cooling.

where $p_{0,i}$ is the ground-state occupation along the i -direction, given by $p_{0,i} = 1 - e^{-\frac{\hbar\omega_i}{k_B T_i}}$. The kinetic energy observed in time-of-flight is half of the total energy and given by

$$K_i = \frac{1}{2} \hbar\omega_i \left(\frac{1}{2} + \frac{1}{e^{\frac{\hbar\omega_i}{k_B T_i}} - 1} \right). \quad (3)$$

This leads to a relative ground state occupation of

$$p_{0,i} = \frac{2}{\frac{4K_i}{\hbar\omega_i} + 1}, \quad (4)$$

and a phase space density given by

$$\text{PSD} = N_1 \prod_{i=x,y,z} \frac{2}{\frac{4K_i}{\hbar\omega_i} + 1} \quad (5)$$

E. Thermalization Rate

At the end of the cooling, the quasi-1D gas tends to be colder in the transverse direction than in the longitudinal one. This happens because the cooling is performed in the direction of tight confinement and relays on thermalization to lower the temperature in the other direction. It is known that at low temperatures thermalization slows down [4], because two-body collisions that can take enough energy to excite the atoms are highly reduced. We can estimate the thermalization rate due to two-body collisions in our system. Neglecting the effects of correlation, we expect a behavior similar to the one shown in Fig. 3 [5]. For our system, thermalization should virtually stop at temperatures near $0.8 \mu\text{K}$, while the

temperature in the transverse direction can get much colder, as mentioned in the main text. Correlations between the atoms will tend to further reduce the thermalization rate at low temperatures. Thermalization can also be achieved by three-body collisions, but this tends to be even further reduced by correlations in a strongly interacting gas, proportional to γ^{-12} . [5].

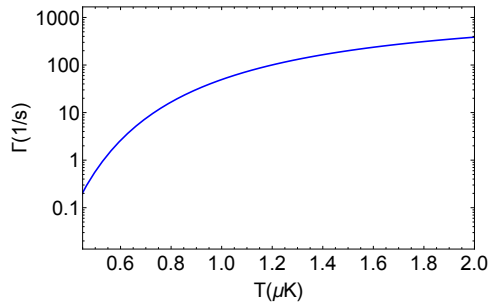


FIG. 3. Thermalization rate as a function of temperature for a quasi-1D gas.

F. Characterization of Time-of-Flight Distributions

We characterize the velocity distribution of the sample using time-of-flight measurements. We let the gas expand for $800 \mu\text{s}$ before an absorption image is taken. We integrate over the vertical or horizontal direction of the image to obtain the velocity distribution along the direction of tight or weak confinement, respectively. We fit a Gaussian distribution to all the data points and then eliminate all the points within one standard deviation of that fit (see Fig. 4). We then fit a Gaussian distribution to the remaining tails. In the direction of tight confinement we always observe a distribution that is well approximated by a Gaussian. On the other hand, the momentum distribution along the direction of weak confinement has a non-Gaussian central part. We consider these characteristic non-Gaussian momentum distributions as a signature of a quantum degenerate gas. We fit the non-Gaussian fraction of the data to a Thomas-Fermi distribution (inverted parabola) with reasonable agreement, although the exact momentum distribution near zero-momentum in general does not have an analytic functional form. However, we can quantify the fraction of atoms that do not follow a thermal distribution by the ratio of the area under the inverted parabola to the total area.

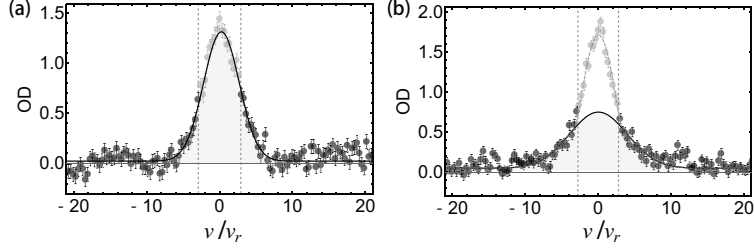


FIG. 4. Velocity distribution of the atoms normalized by the recoil velocity. (a) Velocity distribution along the tightly confined direction, fit to a Gaussian. (b) Velocity distribution along the weakly confined direction. The vertical dashed lines correspond to plus and minus one standard deviation. The solid black curve is the fit to a Gaussian distribution considering only the darker data points and the grey dashed curve in (b) is a Gaussian distribution plus an inverted parabola.

G. Photo-induced Losses and $g^{(2)}$ Correlation Function

In the regime where the loss and temperature change are small, i.e., the average density $\langle n \rangle$ is approximately constant, we can describe the atom number loss due to photo-induced two-body inelastic collisions as an exponential decay determined by the differential equation

$$\dot{N} = -\Gamma N. \quad (6)$$

The loss rate $\Gamma = Gg^{(2)}\langle n \rangle$ depends on the three-dimensional average atomic density $\langle n \rangle$, the photo-association rate constant G , and normalized probability to find two atoms at vanishing interatomic distance $g^{(2)}(\mathbf{r} = 0)$.

The atom-atom correlation function $g^{(2)}$ can be evaluated by comparing densities and decay rates for the cases of one- and two-dimensional gases, by turning on or off one of the trapping lattices. The ratio of $g^{(2)}$ in both cases is

$$\frac{g_{1D}^{(2)}}{g_{2D}^{(2)}} = \frac{\Gamma_{1D} \langle n \rangle_{2D} G_{2D}}{\Gamma_{2D} \langle n \rangle_{1D} G_{1D}}, \quad (7)$$

where the densities can be calculated from the measured atomic average kinetic energy and the trapping frequencies. We fit the data to the solution of Eq. (6) to extract the value of Γ . The quantity $\Gamma_{1D} \langle n \rangle_{2D} / \Gamma_{2D} \langle n \rangle_{1D}$ is shown in Fig. 4a of the main text. If we assume that the two-dimensional gas is approximately thermal, for which $g_{2D}^{(2)} = 2$, we obtain

$$g_{1D}^{(2)} \simeq 0.1 \frac{G_{2D}}{G_{1D}}. \quad (8)$$

In an ideal experiment, the photo-association rates are constant, allowing to extract the value of $g^{(2)}$ for different trap geometries, but in practice they may differ. One possibility explanation for having $G_{1D} \neq G_{2D}$ are the different heating and cooling rates in both configurations, however we measure both rates to be similar in 1D and 2D. We hypothesize that the main mechanism for having $G_{1D} \neq G_{2D}$ is the reduction of on-resonance photo-association due to the tight confinement. Two atoms photo-associate with resonant light if they are separated by a distance close to the Franck-Condon point [6]. In the case of a 1D trap this holds true only for atoms along the z direction, since the transverse confinement length scale is smaller than the Franck-Condon point for our conditions. In 2D, the resonant condition is satisfied for atoms on a circle in the two-dimensional plane. We can calculate the geometrical factor that differentiates the photoassociation rates in 1D and 2D geometries. Assuming Gaussian density distributions in all directions we can calculate the probability of having two atoms at a distance between r_c and $r_c + \Delta$ apart. In 1D this is $P_{1D} \approx \frac{a_{\perp}}{2\pi\sigma_{1D}} \left(\text{Ei} \left(-\frac{(r_c+\Delta)^2}{4\sigma_{1D}^2} \right) - \text{Ei} \left(-\frac{r_c^2}{4\sigma_{1D}^2} \right) \right)$, where a_{\perp} and σ_{1D} are the rms widths in the direction of tight and weak confinement, respectively, ($a \ll \sigma_{1D}$), and Ei is the exponential integral function. Assuming $\Delta > r_c$, this can be further simplified as $P_{1D} \approx \frac{a}{2\pi\sigma_{1D}} \Gamma \left(0, \frac{r_c^2}{4\sigma_{1D}^2} \right)$, where $\Gamma(0, x)$ is the incomplete Euler Gamma function. The same probability in 2D, under the same approximations, gives $P_{2D} \approx \frac{1}{2\pi} e^{-\frac{r_c^2}{4\sigma_{2D}^2}}$. The ratio of these geometric factor that modify the photoassociation rates is $P_{2D} \approx \frac{1}{\pi} e^{-\frac{r_c^2}{4\sigma_{2D}^2}} \left(1 - e^{-\frac{\Delta^2}{4\sigma_{2D}^2}} \right)$. In general Δ is bigger than σ_{2D} , but the number of atoms separated by more than $2\sigma_{2D}$ is small, cutting off the actual value of Δ . This can be written as

$$P_{2D}/P_{1D} = G_{2D}/G_{1D} \approx \frac{\sigma_{1D}}{a} \frac{e^{-\frac{r_c^2}{4\sigma_{2D}^2}}}{\Gamma \left(0, \frac{r_c^2}{4\sigma_{1D}^2} \right)} \quad (9)$$

Considering $r_c \sim \bar{\lambda} = 135$ nm, the transverse confinement of the trap $a_{\perp} = 39$ nm, and a thermal widths $\sigma_{1D} = 475$ nm and $\sigma_{2D} = 550$ nm, all obtained from experimental measurements, we get $G_{2D} \approx 3.6G_{1D}$, then

$$g_{1D}^{(2)} \sim 0.4. \quad (10)$$

For our parameters, the estimated temperature T , normalized to the degeneracy temperature $T_D = \hbar^2 n_{1D}^2 / (2mk_B) = 46$ nK of the repulsive Lieb-Liniger model [7], is $\tau = T/T_D = 26$. For this temperature and $\gamma = 8$ we expect $g_{1D}^{(2)} \approx 0.4$ [7].

We estimate the linear density n_{1D} assuming a thermal Gaussian distribution of atoms, consistent with our system with temperatures above the degeneracy temperature [8]. Although the generated Super-Tonks gas is in a meta-stable state, this state is long lived, and the gas can be approximated as being in thermal equilibrium throughout all experimentally relevant time scales.

H. Three-Body Losses and $g^{(3)}$ Correlation Function

The density evolution of an atomic ensemble in a trap with three-body loss is governed by

$$\dot{n} = -Kn^3, \quad (11)$$

where K is the three-body loss rate coefficient, and n is the local density. This equation can be re-written in terms of total atom number as

$$\dot{N} = -CN^3, \quad (12)$$

where for a harmonic trap the coefficients are related by

$$K = \frac{3^{3/2}}{\rho_{3D}^2} C, \quad (13)$$

where ρ_{3D} is the single-atom peak density in a trap given by

$$\rho_{3D} = \frac{1}{(2\pi)^{3/2} x_0 y_0 z_0}, \quad (14)$$

where x_0 , y_0 , and z_0 are the root-mean-square size of the atomic distribution in each individual trap given by the temperature and the trapping frequencies.

The solution of the differential equations is

$$N(t) = \frac{N_1}{\sqrt{2CN_1^2 t + 1}}, \quad (15)$$

with N_1 being the initial number of atoms in the trap. Since all traps are almost equally filled due to the two-body loss during the preparation, the evolution of total atom number is governed by the same equation. This is the expression we use for our fits to obtain the three-body loss rate (Fig. 4b of the main text).

The three-body loss rate is proportional to the overlap of the wavefunction of three atoms, characterized by the correlation function $g^{(3)}(\mathbf{r} = 0)$. We consider $K = K_0 g^{(3)}$ and compare

the cases for one- and two-dimensional gases, assuming that K_0 is a constant, independent of the dimensionality of the problem. If we also assume that the two-dimensional gas is approximately in a thermal distribution, where $g_{2D}^{(3)} = 6$, then our measurements of three-body loss yields

$$g_{1D}^{(3)} \simeq 0.05. \quad (16)$$

Analogously to $g^{(2)}$, $g^{(3)}$ can be calculated from theory even at finite temperature, and for our parameters ($\gamma = 8, \tau = 22$) is given by $g_{1D}^{(3)} \simeq 0.06$ [7].

The main source of systematic errors for measuring $g_{1D}^{(3)}$ comes from the uncertainty of the atomic density in the case of a 2D traps (1D lattice). We observe neighboring traps getting populated while atoms are held in the dark (without cooling). This effects decreases the density of atoms by a factor of 4, and adds a uncertainty of 50 percent in determining the value of K_{2D} .

-
- [1] K. Shibata, S. Yonekawa, and S. Tojo, [Phys. Rev. A **96**, 013402 \(2017\)](#).
 - [2] J. Hu, A. Urvoy, Z. Vendeiro, V. Crépel, W. Chen, and V. Vuletić, [Science **358**, 1078 \(2017\)](#).
 - [3] A. Urvoy, Z. Vendeiro, J. Ramette, A. Adiyatullin, and V. Vuletić, (2019), [arXiv:1902.10361](#).
 - [4] D. S. Petrov and G. V. Shlyapnikov, [Phys. Rev. A **64**, 012706 \(2001\)](#).
 - [5] I. E. Mazets and J. Schmiedmayer, [New Journal of Physics **12**, 055023 \(2010\)](#).
 - [6] K. Burnett, P. S. Julienne, and K.-A. Suominen, [Phys. Rev. Lett. **77**, 1416 \(1996\)](#).
 - [7] M. Kormos, G. Mussardo, and A. Trombettoni, [Phys. Rev. A **83**, 013617 \(2011\)](#).
 - [8] Y. Hao, Y. Song, and X. Fu, [International Journal of Modern Physics B **30**, 1650216 \(2016\)](#).